MURI-ASAP
Optimal Asset Distribution for Environmental Assessment and Forecasting Based on Observations, Adaptive Sampling, and Numerical Prediction

Dr. Pierre F.J. Lermusiaux – co-PI
Department of Mechanical Engineering, Center for Ocean Science and Engineering,
Massachusetts Institute of Technology
Room 5-207; 77 Massachusetts Avenue
Cambridge, MA 02139-4307
Phone: (617) 324-5172
Email: pierrel@mit.edu

Award #: N00014-04-1-0534 – MIT-sub (00000917)
Web: http://mseas.mit.edu/, http://mseas.mit.edu/Research/ASAP/index.html

LONG-TERM GOALS and OBEJCTIVES

1. Carry out cooperative real-time (sub)-mesoscale data-driven predictions with adaptive sampling and research and evaluate skill measures

2. Advance scientific understanding of 3D upwelling/relaxation dynamics and carry out budget analyses as possible (multi-balances, sensitivity studies, parameterizations, predictability)

3. Determine details of three metrics for adaptive sampling (coverage, dynamics, uncertainties) and develop schemes and exercise software for their integrated use

APPROACH

1. Further modeling system improvements and skill metrics
    a. Re-analyses and Multi-model comparison and combination

2. Ocean Dynamics
    a. AN Budgets, Tidal effects, Eddying off AN shelf, Undercurrent and CC dynamics/interactions, Coastal trapped waves, etc
    b. Study impact of larger-scale effects shown today on AN shelf

3. Data Assimilation (DA), Uncertainty and Predictability Limits
    a. ESSE smoothing for initial conditions
    b. OSSE for adaptive sampling (multi-scale sampling)

4. Multi-Scale Energy and Vorticity Analysis (MSEVA), Scale estimation and LCS for dynamics, sampling and DA

Report Documentation Page

Form Approved
OMB No. 0704-0188

1. REPORT DATE	2. REPORT TYPE	3. DATES COVERED
30 SEP 2008	**Annual**	**00-00-2008 to 00-00-2008**

4. TITLE AND SUBTITLE
Optimal Asset Distribution For Environmental Assessment And Forecasting Based On Observations, Adaptive Sampling, And Numerical Prediction

5a. CONTRACT NUMBER

5b. GRANT NUMBER

5c. PROGRAM ELEMENT NUMBER

6. AUTHOR(S)

5d. PROJECT NUMBER

5e. TASK NUMBER

5f. WORK UNIT NUMBER

7. PERFORMING ORGANIZATION NAME(S) AND ADDRESS(ES)
Massachusetts Institute of Technology,Department of Mechanical Engineering, Center for Ocean Science and Engineering,Room 5-207; 77 Massachusetts Avenue,Cambridge,MA,02139-4307

8. PERFORMING ORGANIZATION REPORT NUMBER

9. SPONSORING/MONITORING AGENCY NAME(S) AND ADDRESS(ES)

10. SPONSOR/MONITOR’S ACRONYM(S)

11. SPONSOR/MONITOR’S REPORT NUMBER(S)

12. DISTRIBUTION/AVAILABILITY STATEMENT
Approved for public release; distribution unlimited

13. SUPPLEMENTARY NOTES
code 1 only

14. ABSTRACT
Carry out cooperative real-time (sub)-mesoscale data-driven predictions with adaptive sampling and research and evaluate skill measures 2. Advance scientific understanding of 3D upwelling/relaxation dynamics and carry out budget analyses as possible (multi-balances, sensitivity studies, parameterizations, predictability) 3. Determine details of three metrics for adaptive sampling (coverage, dynamics, uncertainties) and develop schemes and exercise software for their integrated use

15. SUBJECT TERMS

16. SECURITY CLASSIFICATION OF:			17. LIMITATION OF ABSTRACT	18. NUMBER OF PAGES	19a. NAME OF RESPONSIBLE PERSON
a. REPORT **unclassified**	b. ABSTRACT **unclassified**	c. THIS PAGE **unclassified**	**Same as Report (SAR)**	**6**	

WORK COMPLETED

Real-time Modeling and Dynamics: A manuscript on the HOPS real-time forecasting and re-analysis for AOSN-II was completed and accepted for publication (Haley et al, 2009).

Barotropic Tide Estimation: Resolution, open boundary condition (OBC) schemes, parameterization of the dissipative and non-linear terms in the depth-averaged momentum equations were investigated. These efforts were directed towards understanding the effects of the OBC formulation, frictional and dissipative effects, and non-linear barotropic-to-baroclinic conversions on the barotropic tidal solution. The previously coded Dirichlet conditions at open boundaries have been augmented with the option of having Neumann and mixed OBCs. The sensitivities of the depth-averaged tidal solutions to the type of OBCs have been studied. In addition, various simple parameterization of bottom friction have been implemented. An iterative approximation method has been evaluated to deal with the non-linearity in the dissipation term in the momentum equations. Bottom friction parameters have been estimated using the ADCP velocity data off the coast of Año Nuevo and a fit of the tidal dynamics to data.

Grid interpolation and continuity: The (nontrivial) process of transferring the barotropic tidal fields from their original grid (unrotated Arakawa C-grid) to the dynamical model grid (possibly rotated B-grid) has been upgraded in two distinct areas: the C-grid to B-grid interpolation and the enforcement of the continuity equation. First, the tidal transports are now interpolated not the barotropic tidal velocities. The interpolated transports are then scaled by the dynamical model grid topography to obtain velocities. The second upgrade is in the second step, where an additive correction to the interpolated barotropic velocity is constructed to ensure that the *discrete* barotropic continuity equation is *exactly* satisfied on the *B-grid*. This correction is found by solving a Poisson equation for a velocity potential. The upgrade is the construction of Neumann boundary conditions by integrating the Poisson equation in space and using the divergence theorem to convert the 2D integrals of divergence terms into line integrals of normal derivatives of velocity potential and velocity components around the boundary of the computational domain. The remaining term, the horizontal integral of the time rate of change of surface elevation, is heuristically converted to a boundary integral by fitting a shape function based on the normal components of the interpolated transports. The final boundary condition is obtained by assuming the integrand of the line integral is zero at every boundary point.

Multi-model comparisons: The predictions from the three modeling systems used during MB06 differed because of the different models, initial and boundary conditions, and data assimilation. Our hypothesis based on model comparisons was that difference in larger-scale predictions were mainly due to different initial and boundary conditions. To quantify this, HOPS was initialized with the 2006 NCOM-ICON and ROMS fields and comparisons made using RMS error and Pattern Correlation Coefficient metrics. These re-initialized HOPS simulations were compared to persistence (predictive skill) and to the 2006 HOPS fields (to distinguish IC vs. model effects).

Automated model tuning: Work has started on parameterization estimation methods for complex ocean simulations using HOPS (Heubel, 2008). In particular, skill metrics have been utilized to evaluate the performance of various mixing parameterizations and tidal model setups for MB06.

RESULTS

Real-time Modeling and Dynamics: The real-time modeling during AOSN-II was reviewed and assessed (Haley et al, 2009). During MB06, there were two week- to-10-day long upwelling events.

Two types were observed: one with plumes extending westward at points Ano Nuevo and Sur; the other with a thinner band of upwelled water parallel to the coast and across Monterey Bay. During strong upwelling events, the flows in the upper 10-20m had scales similar to atmospheric scales. During relaxation, kinetic energy became available and led to the development of mesoscale features. At 100-300 m depths, broad northward flows were observed, sometimes with a coastal branch following topographic features. An Anticyclone was often observed in the subsurface fields in the mouth of Monterey Bay. The forecasts were found to have skill out to 2 days, especially near the surface. The reanalysis following the experiment was found to improve both the long-term stability of the simulations and the quantitative skill (especially in the main thermocline where the simulation RMS temperature errors were $1^{o}C$ less than persistence RMS errors, see Haley et al., 2009).

Barotropic Tide Estimation: The diurnal tidal constituents (K1, O1, P1, etc) were found to be sensitive to the type of the OBCs. According to our theoretical and numerical analysis, the sensitivity is related to the fact that the diurnal tidal constituent are sub-inertial in and north of the Monterey Bay basin. The semi-diurnal constituents are super-inertial, leading to an elliptic boundary value problem, and do not exhibit the same level of sensitivity to the type of the OBCs as the diurnal (sub-inertial) constituent. Specifically, in the sub-inertial regime, the boundary value problem that results from the frequency domain tidal depth-integrated shallow water equations forced through the open boundaries is hyperbolic and requires consistent OBCs. If inconsistent OBCs are specified, wave-like adjustments near the open and the adjacent coastal boundaries can arise. These adjustments are sensitive, firstly, to the degree of inconsistency in the OBCs, as well as to the placement of the computational domain boundaries. Figures 1 and 2 show the depth-averaged velocity field [cm/s] of the K1 tidal constituent in the Monterey Bay area. Two types of the OBCs have been specified. Figure 1 corresponds to the computations with the Dirichlet boundary conditions specified at all open boundaries. A wave like velocity field structure is seen near the coastal northern boundary. As the Dirichlet OBC is relaxed to a mixed OBC on the northern boundary (radiation with external data condition in the frequency domain), the solution changes and no longer contains the spurious wave-like signal near the boundary (see Figure 2). This mixed OBC solution compares better with the ADCP data. Further studies of the OBC schemes and parameterization are currently in progress.

Grid interpolation and continuity: The interpolation of tidal transport (instead of velocities) was found to reduce errors in the B-grid continuity equation but not sufficiently. The additive correction with the new Neumann boundary conditions was found to sufficiently reduce the errors in the B-grid continuity equation, even though the resulting matrix was often ill-conditioned. When distributing the integral of the time rate of change of the surface elevation along the boundary (for the Neumann BCs), it was found that working with the real and imaginary parts separately gave superior results to working in complex-space. The tidal fields satisfying the B-grid continuity produce far more stable solutions when used in the HOPS PE model.

Multi-model comparisons: In the twin-experiments aiming to reproduce NCOM-ICON and ROMS using HOPS, it was found that the HOPS simulation initialized with NCOM-ICON fields and forced by NCOM-ICON at open-ocean boundaries remained very close to the NCOM-ICON real-time simulation for at least 5 days, without becoming close to the real-time HOPS simulations. Looking at the statistics in Table 1, the RMS differences for the NCOM-ICON initialized HOPS runs are significantly smaller that for the HOPS initialized runs for all fields examined (temperature, salinity and baroclinic velocity). Similarly the PCC values are significantly larger for the NCOM-ICOM initialized fields. Comparing these numbers to persistence numbers shows that while the NCOM-ICON initialized HOPS fields are closer to the real-time NCOM-ICON, the predictive skill is fading with time, as the RMS differences and PCC values become closer by day 5. A similar twin experiment was run for ROMS, initializing HOPS with ROMS fields. Again, the ROMS-initialized HOPS were found to remain closer (in RMS and in PCC) to the real-time ROMS fields than to the real-time HOPS fields. When comparing the ROMS-initialized HOPS fields to the persistence fields, the RMS errors and PCC values were equivalent. This was attributed to data assimilation jumps occurring in the ROMS real-time outputs. Overall, these results again confirm that at the larger-scales, initial and boundary conditions (in part via the assimilation) drove the model output differences.

Table 1: Skill values from dynamical model simulations

NCOM-HOPS Comparisons. Mean skill values for reproducing NCOM results using indicated initial/boundary conditions, at 0.5 and 5.0 days								
IC/BC Fields	**T**		**S**		**U**		**V**	
	RMS	**PCC**	**RMS**	**PCC**	**RMS**	**PCC**	**RMS**	**PCC**
NCOM	0.2-0.6	0.95-0.6	0.02-0.068	0.95-0.5	5.0-11	0.8-0.45	6-13	0.8-0.25
HOPS	1.3-1.2	0.15-0.15	0.18-2.0	0.05-0.05	13-17	0.08-0	15-19	0.2-0
Persist	0.4-0.7	0.8-0.45	0.028-0.072	0.9-0.35	5.5-14	0.75-0.03	11-15	0.5-0.15
ROMS-HOPS Comparisons. Mean skill values for reproducing ROMS results using indicated initial/boundary conditions, at 0.5 and 5.0 days								
ROMS	0.45-1.1	0.8-0.28	0.07-0.23	0.85-0.05	8-14	0.88-0.33	8.5-16	0.78-0.2
HOPS	1.55-1.5	-0.1-0.1	0.22-0.23	-0.2- -0.1	18-16	0-0	20-18	-0.1-0.2
Persist	0.5-0.95	0.75-0.25	0.08-0.15	0.8-0.35	9.5-14	0.85-0.55	8.5-14	0.78-0.3

Automated model tuning: To apply estimation methods to complex modeling system, forecasts with different model parameterizations are first compared based on skill metrics. The modeling set-up with the best skill can then be chosen automatically as the best model. Such automated model tuning was carried out (Heubel, 2008) for our re-analyses. The quantitative metrics used were the Pattern Correlation Coefficient (PCC) that measure the agreement of patterns in the modeled and measured synoptic scales (variations from a background ocean state, or background average); Root Mean Squared error, an average variation error between observations and simulations; and Bias error, the averaged difference between observations and simulations. Applying these tools to various model setups indicated that the new high-resolution barotropic tidal forcings led to tracer hindcasts that disagreed with in situ data more than tracer hindcasts forced with an older coarser tidal forcing. This confirmed the spurious waves that appeared in tidal fields with Dirichelet-OBCs when the resolution increased. The automated skill metric analysis also provided insight into mixing parameterizations.

IMPACT/APPLICATIONS

This research will contribute to coastal physical oceanography in general and upwelling dynamics in particular. This will increase capabilities of navy operations in these regions, especially the surveillance of transit routes, safety of man-based activities, management of autonomous vehicles, and overall tactical and strategic decision making under uncertainties in sensitive areas.

TRANSITIONS

Interactions and coordination are ongoing with co-PIs and with NRL collaborators of this MURI.

RELATED PROJECTS

Collaborations occur under the ONR grant "Physical and Interdisciplinary Regional Ocean Dynamics and Modeling Systems" (MIT follow-up to N00014-05-1-0335).

PUBLICATIONS

Haley, P.J., Jr., P.F.J. Lermusiaux, A.R. Robinson, W.G. Leslie, O. Logutov, G. Cossarini, X.S. Liang, P. Moreno, S.R. Ramp, J.D. Doyle, J. Bellingham, F. Chavez, S. Johnston, 2009. Forecasting and Reanalysis in the Monterey Bay/California Current Region for the Autonomous Ocean Sampling Network-II Experiment. *Special issue on AOSN-II*, *Deep Sea Research II*. [accepted, refereed].
Heubel, E.V., 2008. Parameter Estimation and Adaptive Modeling Studies in Ocean Mixing. Master of Science in Mechanical Engineering. MIT, 121pp.

Logutov, O.G., 2008. A Multi-Grid Methodology For Assimilation of Measurements into Regional Tidal Models. Ocean Dynamics. [accepted, refereed].

Logutov, O.G. and Lermusiaux, P.F.J., 2008. Inverse Barotropic Tidal Estimation For Regional Ocean Applications. Ocean Modelling, 25, 17-34. [published, refereed]

Ramp, S.R., R. E. Davis, N. E. Leonard, I. Shulman, Y. Chao, A. R. Robinson, J. Marsden, P.F.J. Lermusiaux, D. Fratantoni, J. D. Paduan, F. Chavez, F. L. Bahr, S. Liang, W. Leslie, and Z. Li, 2008. Preparing to Predict: The Second Autonomous Ocean Sampling Network (AOSN-II) Experiment in the Monterey Bay. Special issue on AOSN-II, Deep Sea Research, Part II. [accepted, refereed].

Several presentations and publications are available from the MSEAS web-site. Specific figures are available upon request.

Figures

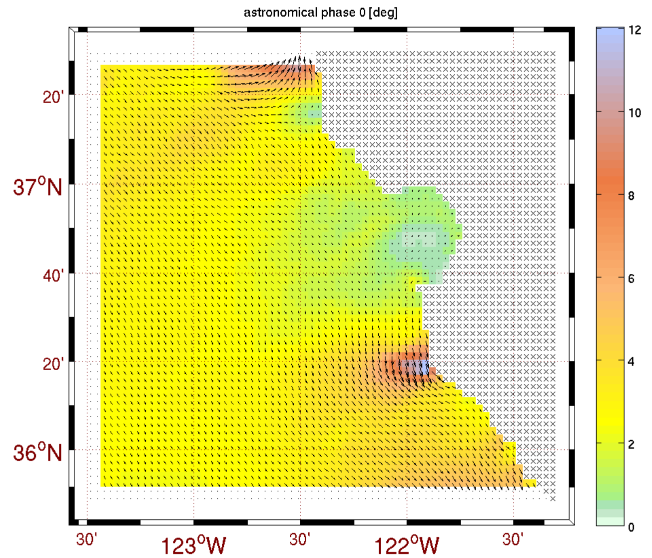

Figure 1: depth-averaged velocity field [cm/s] of the K1 tidal constituent in the Monterey Bay area – Dirichlet boundary conditions specified at all open boundaries

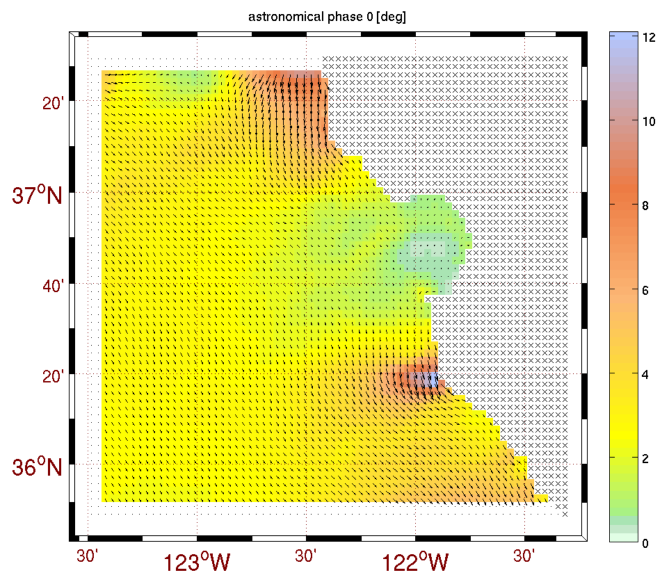

Figure 2: depth-averaged velocity field [cm/s] of the K1 tidal constituent in the Monterey Bay area – absorbing (sponge-like) condition on the northern boundary